

## Electrodeposition of Zinc Oxide NanoSheets on Exfoliated Tips of Carbon Nanotube Films

Erica Freire Antunes<sup>1,a</sup>, Eduardo Saito<sup>1,b</sup>, Matheus Pianassola<sup>2,c</sup>,  
Fernando Henrique Christovan<sup>2,d</sup>, Vladimir Jesus Trava-Airoldi<sup>1,e</sup>  
and Evaldo José Corat<sup>1,f</sup>

<sup>1</sup>Associated Laboratory of Materials and Sensors, National Institute for Space Research,  
Av. Astronautas, 1758, S. José dos Campos, SP, Brazil 12227-010

<sup>2</sup>Department of Science and Technology, Federal University of S. Paulo, R.Talim 330, S. José dos  
Campos, SP, Brazil 12231-280

<sup>a</sup>ericafa2009@hotmail.com, <sup>b</sup>esaito135@gmail.com, <sup>c</sup>pianassola@hotmail.com,  
<sup>d</sup>fhcristovan@unifesp.br, <sup>e</sup>vladimir@las.inpe.br, <sup>f</sup>corat@las.inpe.br

**Keywords:** ZnO nanosheets, carbon nanotubes, electrodeposition, plasma exfoliation, graphene oxide.

**Abstract.** Fast electrodeposition of ZnO nanosheets on exfoliated tips of multi-walled carbon nanotube films by oxygen pulsed DC plasma were investigated. Variation of electrodeposition time showed the presence of ZnO at only 25 s. The dimension of the patterns formed on carbon nanotube films by electrolyte solution controlled the 2D size of ZnO nanosheets. Longer growth produced dense and polycrystalline ZnO nanosheets films but with smaller size by re-nucleation.

### Introduction

Recently, ZnO on graphene and carbon nanotube (CNT) by electrodeposition is a method largely investigated to produce electrochemical detectors [1-2], piezoelectric sensors and nanogenerators [3-4]. The ZnO electrodeposition is based on aqueous solutions of zinc salts [11-13]. Therefore, the wettability behavior of the work electrode is the most important parameter to achieve homogeneous films with an efficient crystal growth.

Originally, CNT and reduced graphene present superhydrophobic character, consequently, attachment of polar groups are needed to improve the electrolyte contact with the work electrode. Several kind of functionalization has been used, based in chemical routes [14], but the most efficient methods concerns about oxygen plasma attack, as shown in our previous work [15,16]. On the other hand, if the graphene sheets had a very high degree of oxidation, the electrical conduction can decrease, and, consequently, electrodeposition will fail.

In this work, the proposal is using vertically aligned multi-walled carbon nanotube (VACNT) films with only their tips made of graphene oxide to grow ZnO nanosheets. For this, we exfoliate VACNT tips, and simultaneously attached functional groups by a treatment with oxygen pulsed DC plasma. This way, the electrical conduction is kept, the VACNT films become superhydrophilic with a high superficial area at the tips for crystal nucleation. Besides, the pattern formed after wetting on VACNT films define the 2D extension of ZnO nanosheets. Here we have showed a new method to electrodeposite ZnO nanosheets directly on VACNT films with fast nucleation and size control by wet pattern dimension and deposition time.

## Experimental Procedure

The electrodeposition of ZnO nanoparticles was run in a AutoLAB equipment using a 0.1M Zn(NO<sub>3</sub>) aqueous solution at a potential of -1.1 V, varying the deposition time from 25 to 480s. The work electrode was made of VACNT films with platinum as counter electrode and Ag/AgCl as reference.

The VACNT films were produced on 1 cm<sup>2</sup> Ti6Al4V square substrates by microwave plasma chemical vapor deposition (MWCVD), with a gas mixture of N<sub>2</sub>/H<sub>2</sub>/CH<sub>4</sub> [12]. A treatment with oxygen plasma in a pulsed DC reactor attached oxygen functional groups on exposed graphene sheets on VACNT tips (O<sub>2</sub>-VACNT) [13]

The morphology of VACNT and ZnO were analyzed by High Resolution Scanning Electron SEM (HR-SEM) from Jeol and TESCAN, with Energy Dispersive X-Ray (EDX) detector. Crystalline structure of ZnO were evaluated by a X-Ray Diffractometer PANalytical X'Pert Powder.

## Results and Discussion

Fig. 1 (a-c) shows SEM images of VACNTs produced by MWCVD grown on Ti6Al4V substrates. Fig. 1a shows the alignment of the tubes, and in Fig.1 (b-c) are details of the VACNT tips exfoliated by O<sub>2</sub>-plasma.

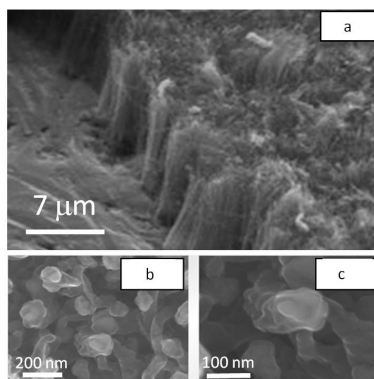


Figure 1 - (a) SEM image of VACNT films grown on Ti substrates; (b, c) detail of the exfoliated VACNT tips.

Fig. 2 (a-c) shows the morphology of ZnO nanoparticles produced at 100, 240 e 480s. An electrodeposition time of 100s produced a homogenous film of micro-sized ZnO nanosheets, while high-density films compounded by smaller crystals were formed for the longest processes.

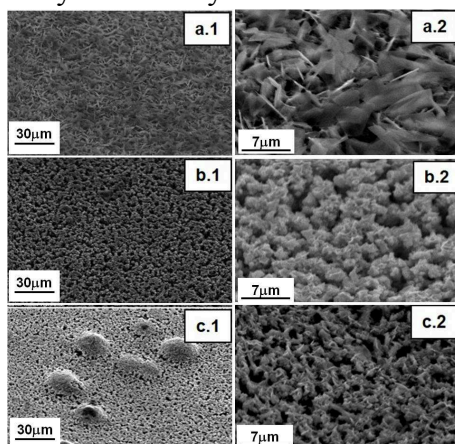


Figure 2 - SEM images of ZnO films grown on O<sub>2</sub>-VACNT by (a) 100 s, (b) 240 s, and (c) 480 s. The numbers 1 and 2 just indicate different magnifications of the same sample.

Conventional SEM images are not capable to detect presence of ZnO crystal at 25 and 50 s. Therefore, HR-SEM images were used to analyze the nucleation of ZnO nanosheets, as shown in Fig. 3. Fig. 3(a-b) shows HR-SEM images of ZnO produced at 50s (a1-a4), and details of ZnO nanosheets produced at 100s (b1-b4) bounded to CNT net.

Fig. 3a1 shows the wettability pattern formed on O<sub>2</sub>-VACNT films after ZnO electrodeposition. The CNT tips have high affinity with water, and they joint themselves due capillary and electrostatic forces during water spreading, as indicated by Fig.3 (a2-a3). Fig.3 (a3-a4) shows the VACNT with a coating, evidencing where the nucleation of ZnO nanosheets starts.

The 2D size of the ZnO nanosheet seems to be defined by the wettability pattern dimension, as shown in Fig. 3b1. Fig. 3 (b2) is a backscattering images, where white region indicates de Zn presence. Notice there are many nanometric bright points for all the image, probably they are new ZnO nucleous. Fig.3b3 shows a detail of the thickness of nanosheet ( $48 \pm 17$  nm), and the Fig. 3b4 shows a detail of the interaction between exfoliated tips of CNT and ZnO nanoparticles

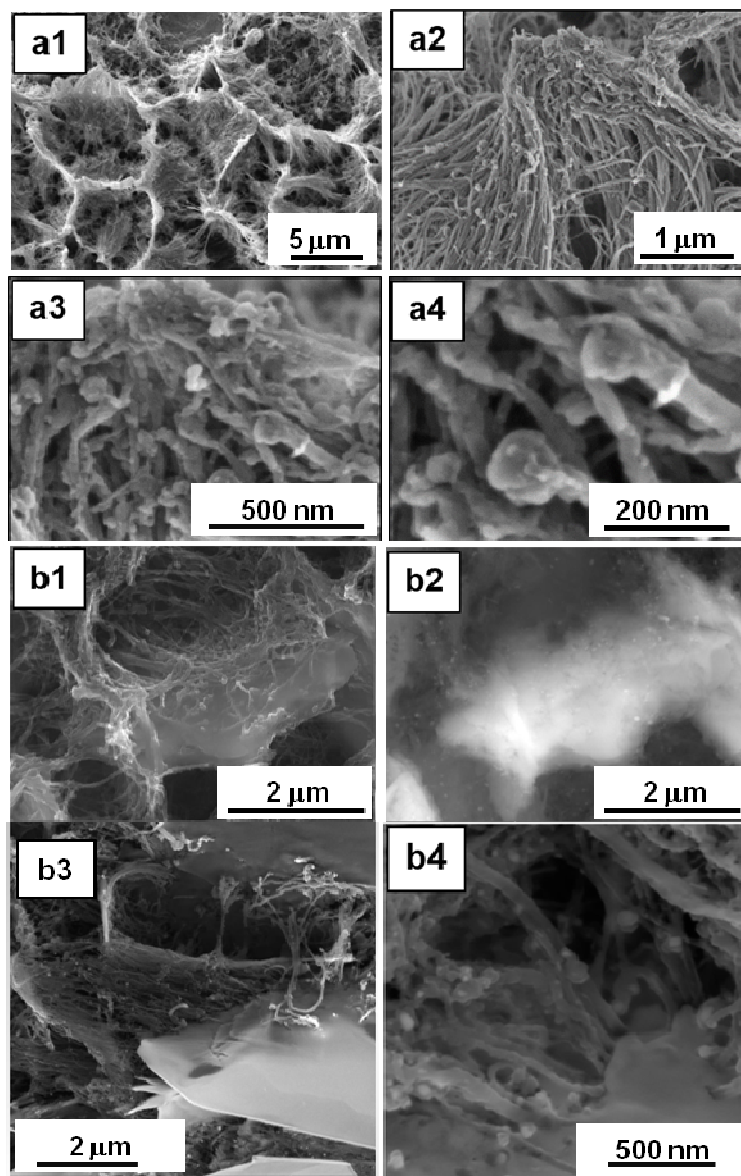


Figure 3 - High resolution SEM images of ZnO coatings deposited in (a) 50 s and (b)100 s.

To prove that O<sub>2</sub>-VACNT tips was really covered by ZnO in early stages of electrodeposition (50 s), an EDX map at 20kV were run. Fig. 4 shows a EDX spectra and map,

which confirms the presence of Al and Ti from substrate, C from CNTs, and also O and Zn from zinc oxide.

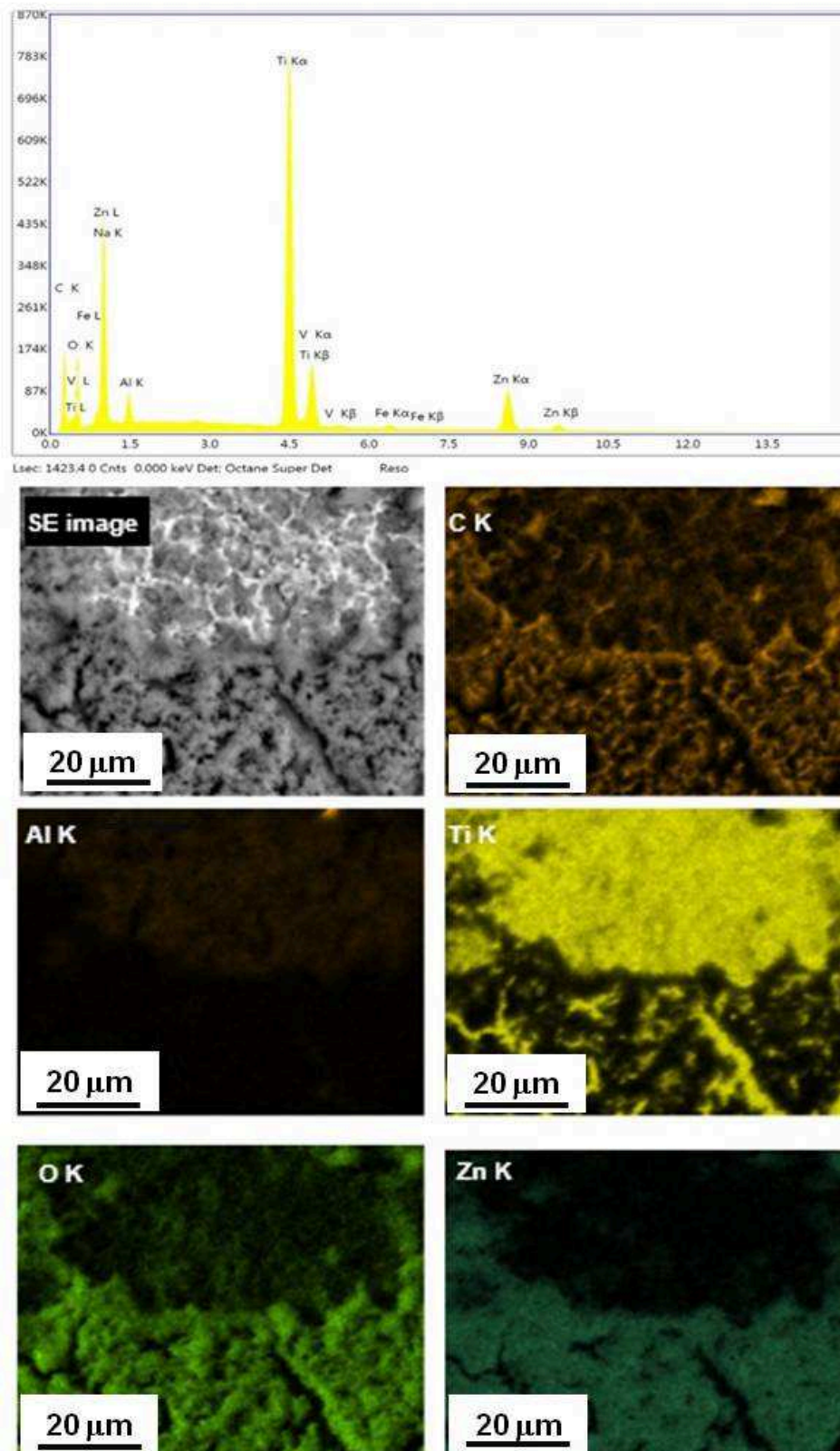


Figure 4 - EDX map of ZnO coating deposited by 50s on O<sub>2</sub>-VACNT/Ti6Al4V

X-Ray diffraction patterns also showed the presence of ZnO peaks even at samples produces at only 25 s (Fig. 5). At total range, the peaks around 31.9, 34.6, 35.6, 36.5, 47.5, 56.5, 62.8, and

67.9, correspond to (100), (002), (101), (102), (110), (103), and (112) planes, respectively. Fig. 5b shows a graph for 2theta from 31 to 38 degrees. At this range, until 100 s of growth, the main peak refers to ZnO (101) with right shift, and after 240 s, more two peaks related to (100) and (101) planes appear (Fig. 5b). It indicates the nanosheets has (101) as preferential plane, when in contact with CNT net, but further nanosheet layer emerged from the first ZnO layers are polycrystalline. Hydroxides like  $\text{Zn}_5(\text{OH})_8(\text{NO}_3)\cdot 2\text{H}_2\text{O}$  can be deposited simultaneously to ZnO. oxides If this happens, an annealing at temperatures around 250 °C by 10 min its enough to convert hydroxide phases to oxide (Fig. 5c).

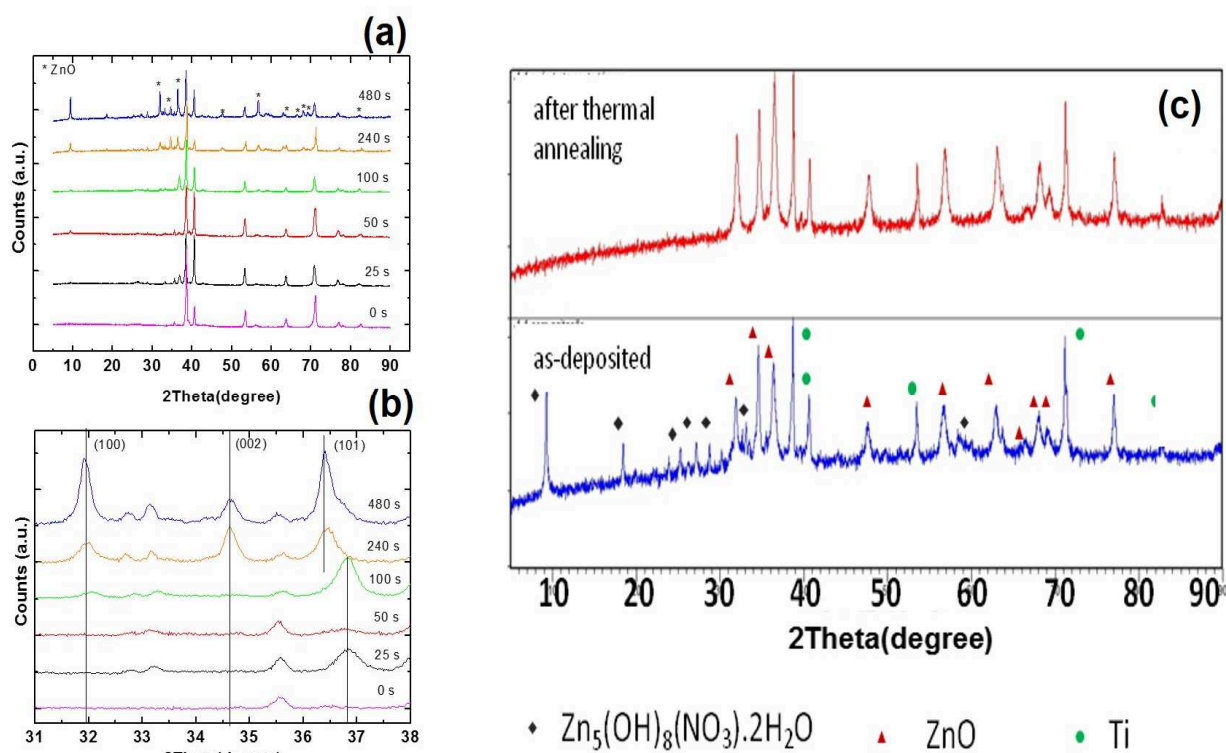


Figure 5 - X-ray diffraction pattern of ZnO/ $\text{Zn}_5(\text{OH})_8(\text{NO}_3)\cdot 2\text{H}_2\text{O}$  coating: (a) total range; (b) details of (100), (002) and (101) peaks, (c) ZnO peaks after annealing at 250 °C.

## Conclusion

The growth of ZnO nanosheets on VACNT films were successful achieved by electrodeposition using zinc nitrate solution, after exfoliation and functionalization by pulsed DC plasma with oxygen. The wettability pattern of VACNT films provides an electric field concentration at their superhydrophilic and jointed tips. Therefore, as the attraction of zinc ions is higher at nanotubes tips, the ZnO preferentially nucleates at this place, and grows limited by the CNT net formed. Changes in size of nanosheets for longer time of growth indicate that a re-nucleation occurs from first ZnO nanosheet layer.

## Acknowledgments

The authors are grateful to Tescan and Jeol for HR-SEM images and to FAPESP/CNPq for financial support

## References

- [1] J. Xu, C. Liu, Z. Wu. Direct electrochemistry and enhanced electrocatalytic activity of hemoglobin entrapped in graphene and ZnO nanosphere composite film, *Microchim. Acta* 172 (2011) 425-430
- [2] S. Palanisamy, A.T. Vilian Ezhil, C. Shen-Ming, Direct electrochemistry of glucose oxidase at reduced graphene Oxide/zinc oxide composite modified electrode for glucose sensor, *Int. J. Electrochem. Sci.* 7 (2012) 2153.
- [3] K.H. Kim , B. Kumar , K.Y. Lee , H.K. Park , J.H. Lee , H.H. Lee , H. Jun , D. Lee , S.W. Kim, Piezoelectric two-dimensional nanosheets/anionic layer heterojunction for efficient direct current power generation, *Sci. Rep.* 3 (2013)2017.
- [4] H. Sun, H. Tian, Y. Yang, D. Xie, Y.-C.Zhang, X. Liu, S. Ma, H.-M. Zhao, T.-L. Ren, A novel flexible nanogenerator made of ZnO nanoparticles and multiwall carbon nanotube, *Nanoscale* 5 (2013) 6117-6123
- [5] N.K. Hassan, M.R. Hashim, Y. Al-Douri, K. Al-Heusee, Current dependence growth of ZnO nanostructures by electrochemical deposition technique, *Int. J. Electrochem. Sci.* 7 (2012) 4625 – 4635
- [6] A. Kathalingam, M.R. Kim, Y.S. Chae, J.K. Rhee, Studies on electrochemically deposited ZnO thin films, *J. Korean Phys. Soc.* 55 (2009) 2476-2481
- [7] T. Yoshida, D. Komatsu, N. Shimokawa, H. Minoura, Mechanism of cathodic electrodeposition of zinc oxide thin films from aqueous zinc nitrate baths, *Thin Solid Films* 451-452 (2004)166-169
- [8] K. Balasubrainian, M. Burghand, Functionalized Carbon Nanotubes, *Small* 1 (2005) 180-192
- [9] L.F. Bonetti, G.C. Rodrigues, L.V. Santos, E.J. Corat, V.J. Trava-Airoldi, Adhesion studies of diamond-like carbon films deposited on Ti6Al4V substrate with silicon interlayer, *Thin Solid Films* 515 (2006)3750379
- [10] S.C. Ramos, G. Vasconcelos, E.F. Antunes, A.O. Lobo, V.J. Trava-Airoldi, E.J. Corat, Wettability control on vertically-aligned multiwalled carbon nanotube surfaces with oxygen pulsed DC plasma and CO<sub>2</sub> laser treatments, *Diamond and Related Mater.* 19 (2010) 752-755
- [11] A.O. Lobo, S.C. Ramos, E.F. Antunes, F.R. Marciano, V.J. Trava-Airoldi, E.J. Corat, Fast functionalization of vertically aligned multiwalled carbon nanotubes using oxygen plasma, *Mater. Lett.* 70 (2012) 89-93.
- [12] E.F. Antunes, A.O. Lobo, E.J. Corat, V.J. Trava-Airoldi, A.A. Martin, C. Veríssimo, Comparative study of first-and second-order Raman spectra of MWCNT at visible and infrared laser excitation, *Carbon* 44 (2006) 2202-2211
- [13] H. Zanin, E. Saito, H.J. Ceragioli, V. Baranauskas, E.J. Corat, Reduced graphene oxide and vertically aligned carbon nanotubes superhydrophobic films for supercapacitor devices, *Mater. Res. Bull.* 49 (2014) 487-493

## Electroceramics VI

10.4028/www.scientific.net/AMR.975

## Electrodeposition of Zinc Oxide NanoSheets on Exfoliated Tips of Carbon Nanotube Films

10.4028/www.scientific.net/AMR.975.50

### DOI References

- [1] J. Xu, C. Liu, Z. Wu. Direct electrochemistry and enhanced electrocatalytic activity of hemoglobin entrapped in graphene and ZnO nanosphere composite film, *Microchim. Acta* 172 (2011) 425-430.  
<http://dx.doi.org/10.1007/s00604-010-0515-x>
- [4] H. Sun, H. Tian, Y. Yang, D. Xie, Y. -C. Zhang, X. Liu, S. Ma, H. -M. Zhao, T. -L. Ren, A novel flexible nanogenerator made of ZnO nanoparticles and multiwall carbon nanotube, *Nanoscale* 5 (2013) 6117-6123.  
<http://dx.doi.org/10.1039/c3nr00866e>
- [6] A. Kathalingam, M.R. Kim, Y.S. Chae, J.K. Rhee, Studies on electrochemically deposited ZnO thin films, *J. Korean Phys. Soc.* 55 (2009) 2476-2481.  
<http://dx.doi.org/10.3938/jkps.55.2476>
- [7] T. Yoshida, D. Komatsu, N. Shimokawa, H. Minoura, Mechanism of cathodic electrodeposition of zinc oxide thin films from aqueous zinc nitrate baths, *Thin Solid Films* 451-452 (2004)166-169.  
<http://dx.doi.org/10.1016/j.tsf.2003.10.097>
- [8] K. Balasubrainian, M. Burghand, Functionalized Carbon Nanotubes, *Small* 1 (2005) 180-192.  
<http://dx.doi.org/10.1002/sml.200400118>
- [9] L.F. Bonetti, G.C. Rodrigues, L.V. Santos, E.J. Corat, V.J. Trava-Airoldi, Adhesion studies of diamond-like carbom films deposited on Ti6Al4V substrate with silicon interlayer, *Thin Solid Films* 515 (2006)3750379.  
<http://dx.doi.org/10.1016/j.tsf.2005.12.154>
- [11] A.O. Lobo, S.C. Ramos, E.F. Antunes, F.R. Marciano, V.J. Trava-Airoldi, E.J. Corat, Fast functionalization of vertically aligned multiwalled carbon nanotubes using oxygen plasma, *Mater. Lett.* 70 (2012) 89-93.  
<http://dx.doi.org/10.1016/j.matlet.2011.11.071>
- [12] E.F. Antunes, A.O. Lobo, E.J. Corat, V.J. Trava-Airoldi, A.A. Martin, C. Veríssimo, Comparative study of first-and second-order Raman spectra of MWCNT at visible and infrared laser excitation, *Carbon* 44 (2006) 2202-2211.  
<http://dx.doi.org/10.1016/j.carbon.2006.03.003>
- [13] H. Zanin, E. Saito, H.J. Ceragioli, V. Baranauskas, E.J. Corat, Reduced graphene oxide and vertically aligned carbon nanotubes superhydrophobic films for supercapacitor devices, *Mater. Res. Bull.* 49 (2014) 487-493.  
<http://dx.doi.org/10.1016/j.materresbull.2013.09.033>